Applied Soil Ecology 80 (2014) 77–83

Contents lists available at ScienceDirect

Applied Soil Ecology

journal homepage: www.elsevier.com/locate/apsoil

Short communication

Reconstructing mole tunnels using frequency-domain ground penetrating radar

Timothy Saey*, Marc Van Meirvenne, Jan De Pue, Ellen Van De Vijver, Samuël Delefortrie

Department of Soil Management, Ghent University, Coupure Links 653, 9000 Gent, Belgium

ARTICLE INFO

Article history:
Received 24 December 2013
Received in revised form 27 March 2014
Accepted 31 March 2014

Keywords:
Mole tunnels
Geophysical detection
GPR
Non-invasive
Earthworm distribution

ABSTRACT

The European mole (*Talpa europaea* L.) inhabits an underground tunnel system whereby the density, extent and condition of the subsurface tunnels are indicative of its activity. Currently, no survey method was able to reveal the spatial extent and condition of the mole's tunnel network. Frequency-domain ground penetrating radar (GPR) was evaluated on its potential to image these shallow tunnel systems. This technique allows for a non-invasive, high-resolution mapping of the subsurface. We examined the effectiveness of this GPR system for delineating the mole's tunnel network. The integration of different depth slices allowed a detailed overview of the tunnel system. Automatic feature recognition on these GPR images was proven valuable for the detection and representation of the mole tunnels. The GPR survey proved successful in mapping the mole's tunnel network, which facilitates the interpretation and characterization of the mole's living environment. This can be linked to the occurrence of earthworms, as the principle food source of the moles, which regulate important ecosystem processes within the soil. This offers new perspectives for the understanding of the mole's habitat.

1. Introduction

The common European mole (*Talpa europaea* L.) creates an extensive systems of permanent and semi-permanent underground tunnels, which it constantly extends (McVean, 1999; Delattre et al., 2006). This subterranean mammal spends almost its entire life in this underground tunnel system, wherein it actively seeks food, eats, makes its nest, sleeps, breeds and rears its young (Quilliam et al., 1971). Godfrey (1955) recorded that these tunnels are generally located several inches below the soil surface. Parameters of burrow systems are affected by environmental factors, particularly availability and distribution of food, soil characteristics and climate, as was defined by Šumbera et al. (2003) for subterranean rodents. It is generally believed that the depth at which digging occurs is related to both the hardness and humidity of the soil and the food supply (Edwards et al., 1999). Shallow tunnels are made when the soil is loosely packed and moist, but when it becomes hard and dry, digging occurs within the deeper soil layers. These shallow tunnels are used to hunt earthworms and insects. In areas of high food availability, a stable tunnel system gives rise to adequate food supply. In areas where food is scarce, moles need to produce new tunnels continually to gain access to sufficient food. Subsequently, the density, extent and condition of the subsurface tunnels can possibly be linked to the presence of earthworms (Edwards et al., 1999). Earthworms play a major role in the regulation of important ecosystem processes such as litter decomposition and nutrient cycling, and in the services delivered by the ecosystem (Valckx et al., 2009). Therefore, if relations between geophysical measurements and earthworm presences could be established, these measurements could be linked to soil ecological processes. However, complex inter-relationships exist between physical, chemical, and biological soil properties and their response to soil ecology (Johnson et al., 2001).

Up to date, only a few studies used non-invasive soil measurements to the detect the presence of soil fauna (Joschko et al., 2010; Valckx et al., 2009). However, no non-destructive method was applied successfully to map the small, air-filled tunnels of the mole. For studying their ecology, a demanding method of uncovering and mapping burrow systems is often used. In the past, burrow systems were excavated, measured and mapped after digitizing, as done by Rosi et al. (2000) for the subterranean rodent *Cyenomys mendocinus*. Spinks et al. (2000) trapped out colonies of the common mole-rat (*Cryptomys hottentotus hottentotus*), after which the entire burrow systems were excavated and mapped on a graph paper. A similar procedure was followed by Šklíba et al. (2012), whereby they identified the position of nests (chambers with bedding), toilets (chambers or blind tunnels filled with feces) and food stores (chambers or blind tunnels with stored food) within the

* Corresponding author. Tel.: +32 9 264 60 42; fax: +32 9 264 62 47.
E-mail address: Timothy.Saey@UGent.be (T. Saey).

http://dx.doi.org/10.1016/j.apsoil.2014.03.019
0929-1393/

excavated burrows of the Ansell's mole rat (*Fukomys anselli*). The most useful method for studying long-term space use of subterranean animals seems to be (radio)telemetry. Šumbera et al. (2008) excavated and mapped burrow systems of subterranean rodents after radio-tracking. Nevertheless, even the most precise radio-tracking data can barely provide comprehensive information on the actual tunnel system size and structure (Šklíba et al., 2009). Le Comber et al. (2002) mentioned the difficulty of mapping mole-rat burrows, and the destructiveness of the most commonly used methods. They indicated the potential of non-destructive techniques for mapping the underground burrow systems. Therefore, we propose to employ a ground-penetrating radar (GPR) as a non-invasive geophysical prospection technique. Kinlam et al. (2007) provided the first intact visual views of large tunnels of the Gopher Tortoise (*Gopherus polyphemus*) employing this technique. They suggested that measuring at very high GPR antenna frequencies (>900 MHz) could potentially be able to discern small burrows. The development of advanced frequency-domain GPR systems, which measure simultaneously at an wide frequency range, should allow to obtain very detailed 3-D information about the composition of both the shallow and deeper subsurface. Hence it shows potential to evaluate the effectiveness of colonization by a mole community by mapping the mole tunnel network. The primary aim of this study was to explore the possibilities of an advanced frequency-domain GPR system to account for the high-resolution mapping of the mole tunnels. Furthermore, an automatic feature detection methodology was evaluated on its potential to delineate the network of mole tunnels.

2. Materials and methods

2.1. Study site

Our study site is situated in the north of Belgium on the Maldegem-Stekene coversand ridge. This ridge consists of wind-blown, coarse sand (according to the USDA textural classification) rich in organic matter with a Podsolic type of soil development (texture: 3.6% clay, 7.4% silt and 89.0% sand). An area of about 600 m^2, that revealed many molehills, was selected on a pasture field (with central coordinates 51°09′57″N and 3°51′39″E). A small subarea of 25 m^2 was selected to perform invasive observation of the mole tunnels. Starting from the different molehills, the trace of the mole tunnels was excavated and digitized employing a DGPS.

2.2. GPR principle

The high-frequent electromagnetic waves emitted by GPR systems obey the Maxwell's Laws (Daniels, 2004), which allow approximating the downward-propagating velocity (v) in soil by:

$$v = \frac{c}{\sqrt{\varepsilon_r}} \quad (1)$$

with c the speed of light in a vacuum, 0.2998 m ns^{-1} and ε_r the relative dielectric permittivity (Jol, 2009).

GPR systems measure the two-way travel time of a signal from the transmitting antenna to a reflecting interface and back to a receiving antenna. Eq. (1) shows that the velocity of the downward-propagating wave depends mainly on ε_r. Therefore, permittivity contrasts cause GPR reflections (Grote et al., 2005) whereby the degree of contrast determines the amplitude of the generated reflections (Leckebusch, 2003). The travel time of the radar wave through each distinct soil layer can be calculated as the difference in arrival times of the reflections from the interface between two materials with a different ε_r. Therefore, the travel time is dependent of both the thickness and depth of the object buried within the soil and v. Inversely, v at each point of the GPR profile can be estimated by the ratio of the difference between the two-way travel times of upper and lower boundary of each layer (Δt) and the known average thickness (d) of each layer:

$$v = \frac{2 \cdot d}{\Delta t} \quad (2)$$

Finally, v can be converted into ε_r according to Eq. (1).

While some part of the GPR wave is reflected back at the reflecting interface, another part is refracted and continuous traveling through the soil until it encounters another reflecting interface (which may be repeated several more times) or until it attenuates. Attenuation is mainly an effect of the conductivity of the soil through which the pulse is passing. A large water content and elevated clay concentrations reduce propagation velocity strongly and cause attenuation of the GPR signal (Neal, 2004). Knowing ε_r and the conductivity (σ), the attenuation at depth z can be estimated by $e^{-\alpha z}$. Hereby α can be considered a measure of the decay of the strength of the initial high-frequent electromagnetic field.

The depth and resolution of the GPR surveys are also dependent on the antenna frequency. High frequency waves suffer more from attenuation than low frequency components (Xavier Neto and Medeiros, 2006). In general, the higher the antenna frequency, the shallower the depth of penetration but the finer the spatial (horizontal and vertical) resolution (Neal, 2004).

To collect GPR reflections, paired antennas (one transmitting and one receiving antenna) are moved along the soil surface in parallel transects. With frequency-domain radar systems one antenna continuously generates propagating radar waves. The second paired antenna records the amplitude and phase shift of the reflected wave, which is a superposition of the continuous reflections from the subsoil. Subsequently, the digitized wave is transformed to time-domain to depict a set of closely spaced reflection profiles. Point source reflections within these profiles originate from individual rocks, metal objects, pipes that are crossed perpendicularly, and a great variety of other smaller things of this sort. They are, in two-dimensional profiles, visible as reflection hyperbolas, even though they were generated from an area-restricted feature in the ground. These hyperbolas are generated because most GPR antennas produce a transmitted radar beam that propagates downward from the surface in a conical pattern, radiating outward as energy travels to depth. Radar energy will therefore be reflected from buried features that are not located directly below the transmitting antenna but are still within the beam of propagating waves (Conyers, 2004).

2.3. Frequency-domain GPR system

We used a stepped-frequency continuous wave GPR and a corresponding antenna array (3d-Radar AS, Trondheim, Norway). This system generates a continuous-wave signal over a bandwidth between 100 MHz and 3 GHz. The amplitude and phase of this signal, modified by any subsurface reflectors, is determined over a user-defined time (dwell time) at every frequency step, and the resulting data set is then inverted from the frequency to the time-domain using an inverse Fourier transform (Linford et al., 2010). By mixing the transmitting and receiving signal in a quadrature mixer, it is possible to determine the deviation between both signals. For every frequency in-between the minimum and maximum frequency, the amplitude and phase shift from the reflecting signal are determined. The width of the frequency step defines the resolution within the frequency-domain and determines, together with the specified frequency range and dwell time, the scan time of an antenna. The advantage of using a frequency-domain system is that a high signal to noise ratio is obtained, while the frequency range

Fig. 1. Stepped-frequency continuous wave GPR mobile measurement configuration with (a) GPR antenna, (b) distance measurement instrument, (c) Geoscope radar unit, (d) differential GPS antenna, (e) GPS unit and (f) rugged notebook.

can be altered according to the soil conditions or the objective of the survey campaign.

2.4. Data processing

A standard processing of the GPR data was applied using the 3-D Examiner software version 2.80. Different processing steps were applied in the following sequence: (i) the inverse fast Fourier transform to convert the frequency-domain data to time-domain profiles, (ii) adjustment of the time-zero to coincide with the soil surface, (iii) background and noise removal, and (iv) migration to transform the 'hyperbola' shaped reflections to point reflections. The data were analyzed by representing them in vertical sections and time slices at distinct time intervals, revealing informative plan-view structures.

2.5. Automatic feature detection

Edge detection is a tool for abrupt feature detection in image processing. This operation highlights straight edges that might be present within the dataset. Changes in the GPR waveform characteristics can be detected as sharp transitions which allows for an automatic feature detection (Pincus et al., 2013). Among the edge detection methods proposed, the Canny edge detector (Canny, 1986) is the most rigorously defined operator and it is widely used. The Canny method identifies edges by looking for local maxima of the image gradient. The gradient is calculated using the derivative of a Gaussian filter. This method is less likely to be fooled by noise and thus able to detect weak edges (Ding and Goshtasby, 2001).

2.6. Isosurface rendering

Visualizing the three-dimensional information in the data set was done by calculating an isosurface of the reflection strength or amplitude envelope. This allows to extract a volumetric body which represents the volume of the mole tunnels (Leckebusch, 2003). The threshold value of the reflection strength defines a maximum number of possible surfaces within the 3-D volume, which are automatically calculated. Then any surface with a value equal to or greater than a certain percentage of the maximum reflection amplitude value was displayed.

3. Results

3.1. Survey details

In this study, the stepped-frequency GPR system was configured to operate over a bandwidth of 300 MHz to 2.5 GHz which were visited in 2 MHz increments with a dwell time of 2 μs. This frequency range was chosen to target shallow soil phenomena. The composite antenna consists of an array of 7 transmitting and 7 receiving antenna elements, creating 13 transmitter–receiver pairs which are separated by a distance of 0.075 m. Although the antenna can be mounted several tens of cm above the soil surface, we towed it within a non-metallic polyethylene sled onto the surface. In this way we reduced the spherical loss of energy above the soil surface, which seriously diminishes the penetration depth and the signal to noise ratio. By driving with our mobile configuration (Fig. 1) along parallel lines, 1 m apart, we obtained a complete coverage of the study area at a horizontal resolution of 0.075 by 0.075 m. It took about 1 h to survey this zone in full-coverage. A distance measurement instrument based on an electro-mechanical odometer was used to ensure constant trace spacing.

3.2. GPR profiles

Fig. 2 shows a 2-D profile of GPR data. Along this profile, a substantial number of reflection hyperbola's were obtained at different two-way travel times of the GPR wave. Each separate hyperbola originates from an individual point feature within the shallow subsoil. They are assumed to be caused by mole tunnels, which are cut perpendicularly by the GPR profile.

3.3. Time slices

The full coverage of the study site allowed the preparation of a 3-D data cube that can be sliced horizontally at any depth. The data were represented in time-domain as depth slices of the reflection magnitude at 0.08 m intervals revealing informative plan-view information about the reflection strength. Assuming a ε_r of 5.0, most subtle features predominantly come across on the time slices between a depth of 0.11 m and 0.19 m. The most informative of the slices within this depth range are shown in Fig. 3. The slices at depths of 0.11 m (Fig. 3a), 0.14 m (Fig. 3b) and 0.17 m (Fig. 3c) were selected for further investigation.

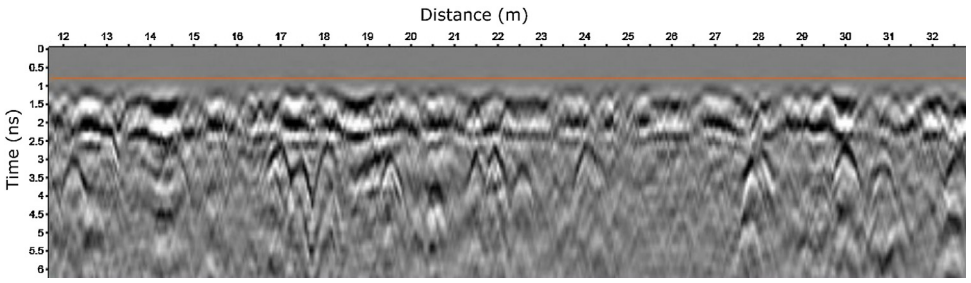

Fig. 2. GPR wave profile as a function of the two-way travel times across the different mole tunnels, expressed as different hyperbola within the profiles.

Fig. 3b clearly shows a network of small positive anomalies across the study site, while Fig. 3a only represents the fragmented onset of the tunnels. Fig. 3c mainly depicts a larger reflection in the central part of the site. One could raise the hypothesis that the connected anomalies originate from a network of mole tunnels. These mole tunnels are cavities within the soil where the air is characterized by a substantially lower ε_r compared to the surrounding soil.

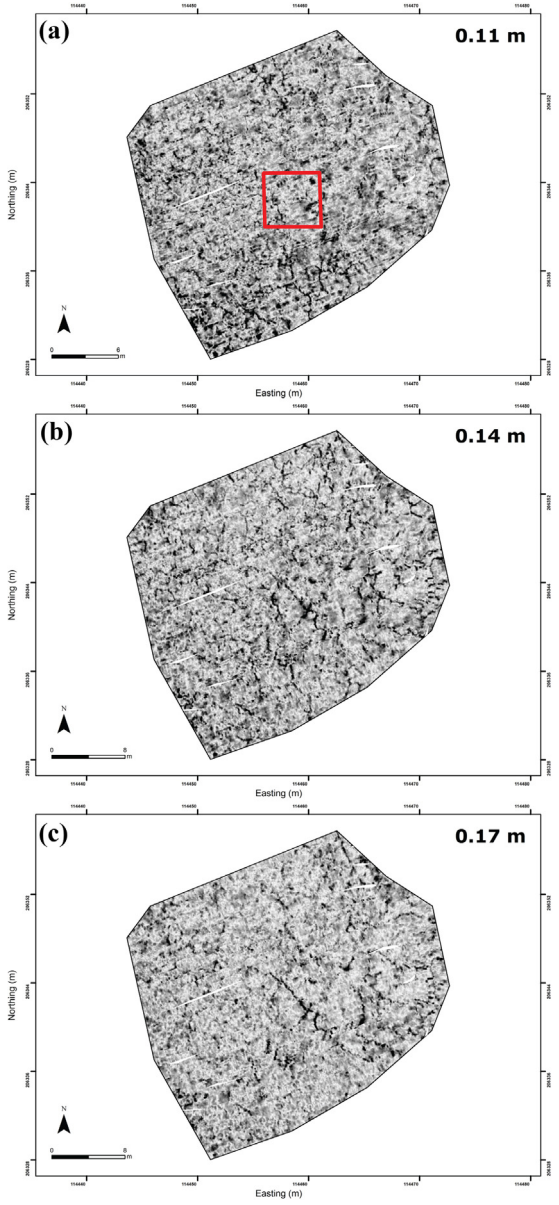

Fig. 3. Depth slices depicting the magnitude of the GPR reflections at a depth of 0.11 m with indication of the mole tunnel verification zone (rectangle) (a), at a depth of 0.14 m (b) and at a depth 0.17 m (c) below the soil surface, focusing on the shallow mole tunnel network.

3.4. Verification

After excavation, the upper boundary of the mole tunnels with an elliptic cross-cut was retrieved at a depth of 0.10 m. This upper boundary, together with the top of the hyperbola within the GPR profiles which was located at a two-way travel time of 1.5 ns, enabled calculating the ε_r of the soil. From Eqs. (1) and (2), a ε_r of approximately 5.0 was deduced. This value was used for both the migration velocity field and the time to depth conversion.

As a verification of the mole tunnel network, we focused on the distinct anomaly that was identified on the depth slices at 0.14 m up to a depth of 0.19 m and selected a subarea of 25 m^2 (Fig. 3a). The result of the excavation draped on the composite depth slice between 0.11 m and 0.19 m is shown in Fig. 4b. Excavation revealed that the continuous anomaly on the depth slices coincided clearly with the main mole tunnel network present in the verification zone, which can be considered a system of continuous tunnels, tens of meter long, at shallow depths. Moreover, no additional mole tunnels were retrieved within this zone. Therefore, we infer that the anomalies visible within this zone all originate from intact and actively used open mole tunnels, which are located at a depth below 0.10 m (at the bottom of the roots of the grass) and with dimensions of 0.08 m (width) by 0.05 m (height). The surface of the entire mole network within the excavated area was calculated to be 1.2 m^2 (=5%), which means that 0.005 m^3 of the subsoil of this area consists of mole tunnels. The discrepancy between the width of the features visible on the GPR slices and the real width makes it impossible to account of the percentage of existing burrows that could be identified by frequency-domain GPR. Nevertheless, the continuity of some mole tunnels could be traced beyond the borders of the excavation zone. The entire network visible on the GPR depth slices at 0.11 m (Fig. 3a) and 0.14 m (Fig. 3b) proved to be a mole tunnel system.

3.5. Automatic feature detection

Fig. 4a shows the results of the Canny edge detection applied on the composite depth slice between 0.11 m and 0.19 m for the excavation zone. The higher threshold of the edge detection algorithm was chosen to be 0.10, which implies the lower threshold to be 0.04. With these thresholds, the delineated edges (Fig. 4a) coincide best with the observed mole tunnel within the excavation zone (Fig. 4b). Some parts of the mole tunnel were however not detected, due to the fact that these parts were less well-established, and therefore less prominent within the subsoil.

To evaluate the accuracies between both the observed mole tunnels and those delineated by the edge detection algorithm on

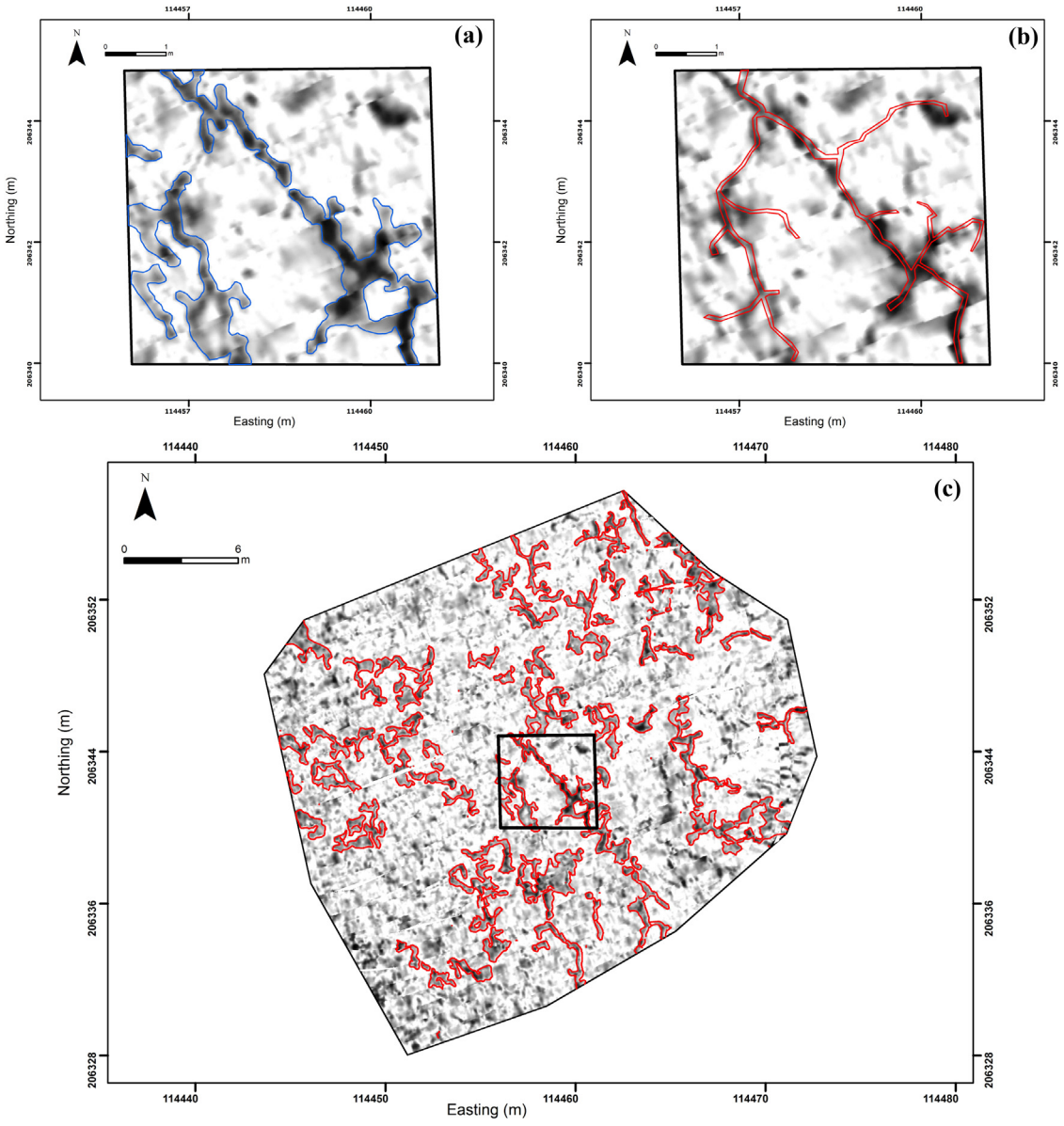

Fig. 4. Composite GPR depth slice at 0.11–0.19 m at the mole tunnel verification zone with indication of the feature delineations (assumed to be the mole network) based on the edge detection algorithm (a) and with the observed mole tunnels (b) and GPR depth slice at 0.11–0.19 m of the entire study site with indication of the feature delineations (assumed to be the mole network) based on the edge detection algorithm (red) and delineation of the verification zone (black) (c). (For interpretation of the references to color in this figure legend, the reader is referred to the web version of the article.)

the combined GPR depth slice, the presence and absence of mole tunnels within both maps (Fig. 4a and b) were compared. The results were summarized in a confusion matrix or contingency table. Two classification accuracy indexes were calculated: overall accuracy rate and the Kappa index between both maps. The former is a simple ratio between the correctly allocated number of pixels (confusion matrix diagonal) and the overall number of classified pixels. The Kappa index is a robust index which takes into account the probability that a pixel is classified by chance. The Kappa index is, therefore, always lower than the overall accuracy measurement (Grinand et al., 2008). The values of overall accuracy (0.82) and Kappa index (0.23) suggest that the correspondence between the mole tunnels delineated by the edge detection algorithm and the observed mole tunnels is fairly good.

Fig. 4c shows that by employing the edge detection algorithm for the entire study site, patterns of small anomalies can be connected to represent a network of mole tunnels.

3.6. Isosurface rendering

The isosurface of the 3-D data of the excavated subarea of the study site is shown in Fig. 5. Although the large anomalies could be easily distinguished from the isosurface, the smaller, more subtle anomalies were impossible to connect to form a continuous network of mole tunnels.

4. Discussion and conclusions

This high-resolution GPR has the ability to distinguish shallow, small features, which experience a distinct permittivity contrast with their surroundings. Within the shallow GPR depth slices, the greater part of the mole tunnels stand out as prominent reflections compared to the surrounding soil, because the air-filled voids provide excellent permittivity contrasts with their surroundings. By integrating multiple slices, the continuous network of tunnels could be identified. The most restrictive condition

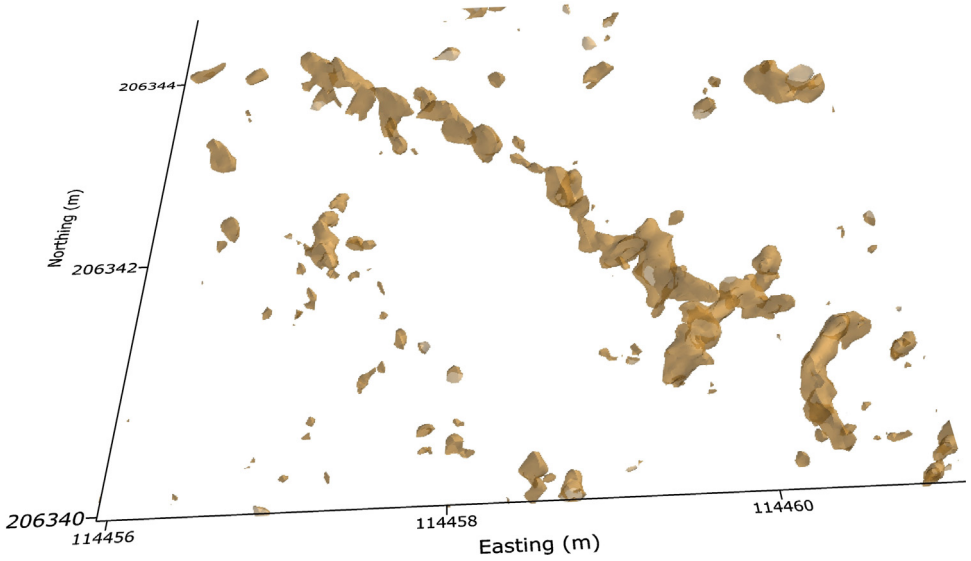

Fig. 5. Isosurface of GPR reflection strength at the mole tunnel verification zone.

to detect small subsurface features at shallow depths is the horizontal resolution, defined as the fineness of the spatial detail visible in the image. In GPR evaluations, it is usually considered as the ability to detect lateral changes or the capacity to detect two close elements at the same depth as two separate anomalies (Pérez-Gracia et al., 2008). The higher frequencies in the spectrum (>2000 MHz) clearly allow distinguishing between separate mole tunnels. Therefore, the system's success in delineating mole tunnels is assumed to decrease substantially with increasing depth, because at lower frequencies the potential to discriminate a single mole tunnel decreases. Moreover, increasing moisture and clay content of the soil increases the attenuation of the GPR wave.

To automatically detect and visualize the tunnel systems in the soil, edge detection on the GPR slices proved to be successful. However, one could observe a discrepancy between the width of the features that were geophysically detected (0.3 m) and the real width (0.1 m). This is possibly due to the fact that the radiated antenna beam has the shape of a wide cone, which means that the antenna detects the tunnels not only when it is directly located above it, but also in several scans before and after the center of the mole tunnels. Another possibility could be that migration was not performed perfectly. The center of the hyperbola remained too wide after migration. Across the entire study site, the mole tunnels in the central and southern part are most prominent. Within the southwestern and northeastern parts, a large number of separated anomalies appears, which is more difficult to interpret as a clear pattern of mole tunnels. It is possible that these anomalies reflect an area without distinct mole tunnels or that the tunnels have been largely collapsed. The isosurface rendering does not provide valuable information about the mole tunnel network. This is mainly due to the lower signal-to-noise ratio at larger depths and because mole tunnels are mainly a 2-D phenomenon. Due to a significantly varying reflection strength, the different parts of the mole tunnels can impossibly be connected: they might be separated during the calculation of the isosurface with a loss of connectivity in the outcome.

To conclude, we successfully applied a frequency-domain GPR to reconstruct a shallow system of mole tunnels in a sandy, dry soil. The approach yielded time-effective and non-invasive insight into the horizontal and vertical extent of the tunnels. Moreover, it does not destroy the burrows, which brings with it the opportunity for repeated measurements of the burrow geometry. Any approach to modeling changes of tunnel structure over time requires for a non-invasive, repeatable and relatively quick method (Kinlam et al., 2007). Although the destructive method of excavating and digitizing the tunnel network destroys the natural habitat of the subterranean mammal, it has the advantage that a more detailed and comprehensive overview of the mole's underground environment can be obtained. This enables a thorough understanding of the burrow architecture of subterranean animals (Šklíba et al., 2012), and their relationship with the surrounding soil characteristics and climatic conditions (Šumbera et al., 2008). Notwithstanding this, one must be careful with the extensive application of destructive methods, because these can cause abandonment or behavioral disruption of the burrow inhabitants. However, excavating and interpreting a small part of the tunnel network can be considered essential to interpret and complement the GPR data. Frequency-domain GPR mapping can also be considered as an alternative for radio-tracking, which has its limitations in discovering the entire underground tunnel network because substantial parts of the network are rarely or never occupied by the radio-tracked animals (Šklíba et al., 2012). A well-considered integration of both GPR and burrow excavation could therefore enhance the full understanding of the driving mechanisms behind the location and density of the burrow systems and the mole's behavior. Further studies on aspects of food availability and its distribution in habitats of moles may reveal intriguing relationships between parameters of food supply and sociality across the moles, or to relate the distribution of mole tunnels to the within-field distribution of earthworms, which are the primary food source of the mole. These results demonstrate the potential of high-resolution, stepped-frequency GPR in resolving questions about the subsurface environment which could be potentially correlated to important soil ecosystem processes. Further investigation that aim at understanding the complementary interactions between the soil biological community and the soil environment should therefore acknowledge geophysical prospection as a valuable tool.

Acknowledgement

The authors would like to thank Valentijn Van Parys for his assistance with the field work.

References

Canny, J., 1986. A computational approach to edge detection. IEEE Trans. Pattern Anal. Mach. Intell. 8, 679–698.

Conyers, L.B., 2004. Ground-Penetrating Radar for Archaeology. Rowman & Littlefield Publishers Inc., Oxford, UK.

Daniels, D.J., 2004. Ground Penetrating Radar. The Institution of Electrical Engineers and Technology, London, UK.

Delattre, P., Clarac, R., Melis, J.P., Peydell, D.R.J., Giraudoux, P., 2006. How moles contribute to colonization success of water voles in grassland: implications of control. J. Appl. Ecol. 43, 353–359.

Ding, L., Goshtasby, A., 2001. On the Canny edge detector. Pattern Recogn. 34, 721–725.

Edwards, G.R., Crawley, M.J., Heard, M.S., 1999. Factors influencing molehill distribution in grassland: implications for controlling the damage caused by molehills. J. Appl. Ecol. 36, 434–442.

Godfrey, G.K., 1955. A field study of the activity of the mole (*Talpa Europaea*). Ecology 36, 678–685.

Grinand, C., Arrouays, D., Laroche, B., Martin, M.P., 2008. Extrapolating regional soil landscapes from an existing soil map: sampling intensity, validation procedures, and integration of spatial context. Geoderma 143, 180–190.

Grote, K., Hubbard, S., Harvey, J., Rubin, Y., 2005. Evaluation of infiltration in layered pavements using surface GPR reflection techniques. J. Appl. Geophys. 57, 129–153.

Johnson, C.K., Doran, J.W., Duke, H.R., Wienhold, B.J., Eskridge, K.M., Shanahan, J.F., 2001. Field-scale electrical conductivity mapping for delineating soil condition. Soil Sci. Soc. Am. J. 65, 1829–1837.

Jol, H.M., 2009. Ground-Penetrating Radar: Theory and Applications. Elsevier Science, Amsterdam, The Netherlands.

Joschko, M., Gebbers, R., Barkusky, D., Timmer, J., 2010. The apparent electrical conductivity as a surrogate variable for predicting earthworm abundances in tilled soils. J. Plant Nutr. Soil Sci. 173, 584–590.

Kinlam, A.E., Conyers, L.B., Zajac, W., 2007. Use of ground-penetrating radar to image burrows of the Gopher Tortoise (*Gopherus polyphemus*). Herpetol. Rev. 38, 50–56.

Leckebusch, J., 2003. Ground-penetrating radar: a modern three-dimensional prospection method. Archaeol. Prospect. 10, 213–240.

Le Comber, S.C., Spinks, A.C., Bennett, N.C., Jarvis, J.U.M., Faulkes, C.G., 2002. Fractal dimension of African mole-rat burrows. Can. J. Zool. 80, 436–441.

Linford, N., Linford, P., Martin, L., Payne, A., 2010. Stepped frequency ground-penetrating radar survey with a multi-element array antenna: results from field application on archaeological sites. Archaeol. Prospect. 17, 187–198.

McVean, A., 1999. Are the semicircular canals of the European mole, *Talpa Europaea*, adapted to a subterranean habitat? Comp. Biochem. Physiol. 123, 173–178.

Neal, A., 2004. Ground penetrating radar and its use in sedimentology: principles, problems and progress. Earth-Sci. Rev. 66, 261–330.

Pérez-Gracia, V., González-Drigo, R., Di Capua, D., 2008. Horizontal resolution in a non-destructive shallow GPR-survey: an experimental evaluation. NDT & E Int. 8, 611–620.

Pincus, J.A., de Smet, T.S., Tepper, Y., Adams, M.J., 2013. Ground-penetrating Radar and electromagnetic archaeogeophysical investigations at the Roman legionary camp at Legio, Israel. Archaeol. Prospect. 20, 175–188.

Quilliam, T.A., Clarke, J.A., Salsbury, A.J., 1971. The ecological significance of certain new haematological findings in the mole and hedgehog. Comp. Biochem. Physiol. 40, 89–102.

Rosi, M.I., Cona, M.I., Videla, F., Puig, S., Roig, V.G., 2000. Architecture of *Ctenomys mendocinus* (Rodentia) burrows from two habitats differing in abundance and complexity of vegetation. Acta Theriol. (Warsz.) 45, 491–505.

Šklíba, J., Mazoch, V., Patzenhauerová, H., Hrouzková, E., Lövy, H., Kott, O., Šumbera, R., 2012. A maze-lover's dream: burrow architecture, natural history and habitat characteristics of Ansell's mole rat (*Fukomys anselli*). Mammal. Biol. 77, 420–427.

Šklíba, J., Šumbera, R., Chitaukali, W.N., Burda, H., 2009. Home-range dynamics in a solitary subterranean rodent. Ethology 115, 217–226.

Spinks, A.C., Bennett, N.C., Jarvis, J.U.M., 2000. A comparison of the ecology of two-populations of the common mole-rat *Cryptomys hottentotus hottentotus*: the effect of aridity on food, foraging and body mass. Oecologia 125, 341–349.

Šumbera, R., Burda, H., Chitaukali, W.N., Kubová, J., 2003. Silvery mole-rats (Heliophobius argenteocinereus Bathyergidae) change their burrow architecture seasonally. Naturwissenschaften 90, 370–373.

Šumbera, R., Šklíba, J., Elichová, M., Chitaukali, W.N., Burda, H., 2008. Natural history and burrow system architecture of the silvery mole-rat from *Brachystegia* woodland. J. Zool. 274, 77–84.

Valckx, J., Cockx, L., Wauters, J., Van Meirvenne, M., Govers, G., Hermy, M., Muys, B., 2009. Within field spatial distribution of earthworm populations related to species interactions and soil apparent electrical conductivity. Appl. Soil Ecol. 41, 315–328.

Xavier Neto, P., Medeiros, W.E., 2006. A practical approach to correct attenuation effects in GPR data. J. Appl. Geophys. 59, 140–151.